41st Aerospace Sciences Meeting and Exhibit
6-9 January 2003, Reno, Nevada

AIAA 2003-311

# Towards Engineering LES of Reacting Flows: Artificial Neural Networks for Efficient Kinetics Modeling.

R. Kapoor*, V. Sankaran† and S. Menon‡
*School of Aerospace Engineering*
*Georgia Institute of Technology*
*Atlanta, Georgia 30332*

Accurate prediction of pollutant emission from combustion devices requires a comprehensive numerical model that can predict not only the unsteady flame structure and propagation characteristics but also pollutant formation. Although flame-turbulence interactions and its effect can be studied using simplified models (e.g., thin-flame), prediction of emission requires detailed finite-rate kinetics. Since chemical kinetics are stiff in time, techniques that can speedup the computations are critically needed. Here, the use of Artificial Neural Network (ANN) for efficient storage and retrieval of chemical composition in a LES, is explored.

## Introduction

Production of pollutants such as carbon monoxide ($CO$) and oxides of nitrogen ($NO_x$ in combustion devices (e.g., gas turbine and internal combustion engines) is becoming a serious concern for environmental reasons and therefore, methods to suppress or eliminate these emissions are being explored. Since, in most experimental cases emission measurements are extractive, the details of when and why combustion process produces $CO$ and $NO$ cannot be directly determined. An accurate simulation methodology, if it exists, would go a long way towards helping the design on next generation low-emission combustors by providing insight into the combustion process, including pollutant formation. Although computational methodology based on large-eddy simulation (LES) has been demonstrated recently as an effective tool to study flame-turbulence interactions,[1–4] the ability to predict multiple chemical species formation in the combustor is still constrained by the computational cost required to track all these species in both space and time. Spatio-temporal resolution of all chemical species in a combustor device operating under real conditions is beyond the current and future processing capability even when massively parallel systems are employed for the simulation.

Therefore, various methodologies are being developed and explored to reduce the cost of computing multi-component species. Methods based on flamelet library,[5] Intrinsic Low Dimension Manifold (ILDM),[6] look-up table (LUT),[7] and In-Situ Adaptive Tabulation (ISAT)[8] have been demonstrated in steady-state Reynolds Averaged Navier-Stokes (RANS) models. More recently, some of these methods have been also used in both time-accurate DNS and LES approaches. The computational efficiency, the accuracy and the ability of these methods are obviously limited by the inherent assumptions used to develop these models. At this time, no method has proven universal for general purpose application.

Here, we are interested in developing a computationally efficient method to simulate detailed chemical kinetics in DNS/LES methodologies. In order to do this, a key feature has to be explicitly addressed. For example, in both DNS and LES multiple flow-through-time ($\tau$) of the flow is simulated to obtain data for reliable stationary statistics. At the minimum, at least 2-3$\tau$ is needed (after the initial transients, typically, 1-2$\tau$, are washed out) to obtain reliable first moment statistics but additional $2-3\tau$ may be needed to obtain second and higher-order statistics. Therefore, the computational cost of DNS or LES is primarily related to the total number of $\tau$ that is needed to address the issue(s) of interest.

From the chemical kinetics calculation point of view after the first 2-3$\tau$ the flow field should (in the mean) settle down and therefore, the accessed composition space should be well established. Therefore, a methodology that stores the composition during the initial stage of evolution and then retrieves this composition during subsequent flow through times should drastically reduce the overall computational cost. Methods that employ direct lookup,[7,9] ISAT[8] or ANNs[10–14] all have potential for providing computational speedup. Recent studies[15] suggest that although ISAT speeds up the chemical species evaluation by a factor of 30-50 (over direct integration), the ISAT table continues to grow (via direct integration) during multiple $\tau$ simu-

*Graduate Research Assistant
†Graduate Research Assistant
‡Professor, AIAA Associate Fellow

lation and can cause potential local memory problems in parallel system.

ANN has been demonstrated as an alternative method to store and retrieve the thermo-chemical state during the simulation. In the past, ANNs have been successfully used in complex system modeling in the fields of electrical engineering and computer engineering, noise and image data pattern recognition, nonlinear controls and forecasting.[16] In combustion related applications, several ANN models have been used in the past. Chemical changes over time for a $H_2/CO_2$ turbulent diffusion flame are predicted using ANN models in a velocity-scalar joint pdf equation model.[11] The simulations have shown good predictions of the flow field and the flame characteristics, when compared to the conventional DI and LUT approaches. The sensitivity and quality of the results to the ANN parameters (number of neurons) is also discussed. Another integrated PDF/neural network approach by Christo *et al.*[10] for a simple one-step chemical reaction has been performed for a non-premixed turbulent flame simulation. Optimized techniques for generating training sets for the networks are discussed.

Blasco *et al.*[12] demonstrated the use of multiple ANNs for simulating the temporal evolution of reactive scalars using a reduced methane-air chemical model involving a four step chemical mechanism with eight species.[17] Multiple ANNs for the prediction of scalars and density and temperature were employed and detailed analysis of the resultant network error was reported. In a later study,[13] the time step was included as an input to the network for modeling, and the ANNs was subdivided on the basis of the accessed compositional domain. The advantage of doing so is in the increased sensitivity of the network output, and the resultant outputs, which are more accurate. Chen *et al.*[14] implemented ANNs using input data for the compositional domain from precalculated ISAT records. The argument is that since ISAT is a better representation of the accessed compositional domain for a reactive system, an ANN trained on such a table will perform with better accuracy. The ANNs were tested in an online partially-stirred reactor calculation. The tremendous advantage of ANN in terms of storage and speedups is demonstrated in this research.

More recently, Kapoor *et al.*[18] demonstrated the use of multiple ANNs for a 15-step, 19-species $CH_4$-air mechanism in a simulation of turbulence-chemistry interactions in the thin-reaction and the flamelet regimes. ANN predictions seem to predict well the flame-broadening effect due to the interaction of small eddies with the flame, as observed in previous work.[15] Later studies[19] also demonstrated the viability of using multiple ANNs to predict outside of the composition domain in which each had been originally trained.

The major advantage of an ANN structure is in terms of the tremendous reductions in CPU times (as opposed to direct integration methods) and disk storage (as opposed to the conventional search/retrieve algorithms). The choice of the correct ANN variables and structure, however, is a critical factor that defines the efficiency and accuracy of the resulting ANN. Furthermore, the true test of the accuracy and efficiency of the ANNs can only be accomplished by employing them in actual multi-dimensional simulations using DNS and/or LES. In this paper, we discuss the development and application of ANNs for multi-step, multi-species mechanisms. Application of these mechanisms in DNS/LES of flame-turbulence interactions is demonstrated, and the accuracy and efficiency of the ANN approach is determined.

## Artificial Neural Network Structure

An ANN structure, by definition, is a structure of several interconnected nonlinear elements, which functions like biological neurons with an ability to learn from a set of input-output parameter space it is subjected to, and then, predict the output for a new sample set with a sufficient level of accuracy.[16] The information in a network is stored in the form of weights and biases (or neurons), which are computed iteratively in the learning phase of the network training.

The inherent capabilities of ANN to model highly complex nonlinear processes makes it a suitable choice to model nonlinear behaviors of temperature and species concentrations in a chemical reaction. There are several training and learning algorithms present in literature, with the option of one or more than one layer of neurons in the network for the same. In general, a perceptron learning rule is favored for our applications, since it is generally robust in its ability to generalize from its training vectors and learn from initially randomly distributed connections.[20]

Mathematically, the output for a multi-layer perceptron (MLP) network can be represented as :

$$Y_i^L = F\left(\sum_{j=1}^{n_L} w_{ij}^L O_j^{L-1} + \beta_i^L\right) \quad for \quad i = 1, ..., n_L \quad (1)$$

where $Y_i^L$ is the output of the $i$th neuron of the $L$th layer, $w_{ij}^L$ represents the weight value for the connecting $j$th neuron of the ($L$-1)th layer and the $i$th neuron of the $L$th layer, $\beta_i^L$ is the bias value, $n_L$ is the total number of neurons in the $L$th layer, and $F$ is the transfer function. Hyperbolic-tangent function is used as the transfer function most commonly. Figure 1 shows the typical layout of a three layer neural network, that has been used significantly in the current work.

The accuracy of the obtained network when used in an online chemistry simulation problem, depends critically on several pre-processing aspects of the network. These are summarized as follows :

- The generation of an initial data set for training the network: This is the most important step in the generation of a useful network for computations. The data bank to be used for the training should ensure that it completely covers the accessed compositional space it will encounter.

- Preconditioning of the training data set for optimal performance: In order to have better network behavior, three different pre-processing steps are followed:

  - Re-scale the variables to achieve zero mean and unit variance,

$$x_i^{'} = \frac{x_i - \tilde{x_i}}{\sigma_{x_i}} \tag{2}$$

    here $x_i$ is the value of the input/output variable $i$ (species mass fraction or temperature) and $\tilde{x_i}$ and $\sigma_{x_i}$ are respectively, the mean and variance of the input/output variable $i$.

  - Re-arrange the input/output sets to fall in the [-1,1] interval. The normalized [-1,1] range has proven to be an optimized range for the ANN training. Thus, a linear transformation has been applied to the initial data-set so as to allow it to fall in the above mentioned range.

$$x_i^{''} = -1 + 2\frac{x_i^{'} - min(x_i^{'})}{max(x_i^{'}) - min(x_i^{'})} \tag{3}$$

    here $max(x_i^{'})$ and $min(x_i^{'})$ denote the maximum and minimum of the standardized values of input (or output) $i$ within the training-set data, respectively.

  - Apply appropriate transformation to the training set to make the training surface well-behaved. This is particularly important in highly temperature sensitive regions where small changes in temperature can result in large production of short-lived radicals. In order for ANNs to predict the chemical state such rapid variations must be included properly. Here, logarithmic and linear transformations are employed.

- The training of the network using a suitable neural net algorithm: In the present work, a multi layer perceptron (MLP) is chosen for the network. It is a supervised, feed-forward neural network, with the architecture described by Eq. 1. Two kinds of learning algorithms have been incorporated: a three-layer scaled conjugate gradient (SCG) back-propagation network[20, 21] and the more popular Levenberg-Marquardt back-propagation network.[20, 22]

- The generation of a validation data set to check the accuracy of the final ANN for sample points not used in the training: The obtained network is tested for accuracy for not only the points it has been trained for but also for the unknown points that exhibit patterns similar to the trained input-output sets.

- The incorporation of the ANN in a real computational simulation: The application of ANNs into a DNS/LES study is the final test of its ability to reproduce the temporal evolution of a chemical system. The accrual of local error after every time step is estimated to quantify the accuracy of the ANNs.

## Results and Discussion

Here, we discuss two applications of the ANNs. Application where the ANNs were used primarily to provide the chemical composition for a given input state is denoted Laminar ANN (LANN) whereas, ANNs which includes turbulent field in addition to the chemical composition is denoted Turbulent ANN (TANN). The applicability of these types of ANNs is discussed below.

### Laminar Artificial Neural Network (LANN)

For the present study, only methane-air mechanisms are employed and ANNs are generated for single-step and multi-step finite-rate mechanisms.

*Global single-step kinetics*

A single-step global mechanism proposed by Westbrook and Dryer[23] involving five species ($CH_4$,$O_2$,$CO_2$,$H_2O$ and $N_2$) is used to develop the simplest LANN. The temporal evolution of any reactive scalar $y_i$ is given in the form

$$\frac{dy_i}{dt} = \dot{\omega}_i(y, T, P) \tag{4}$$

The energy equation can also be written in a similar fashion for the temporal variation of temperature. At present, the time step of the simulations is kept constant in the LANN. Each of the data-set for the training and generation of the laminar nets is pre-processed, as discussed in the previous section. After performing the logarithmic transformations, the data-sets are discretized into different bins based on the input temperature. Each ANN is a three-layer Levenberg-Marquardt back-propagation network, with the number of neurons varying between 15 to 30 in the two hidden layers. The choice of the number of layers and number of neurons in each layer is an open question, and in the present study has been optimized iteratively. Tan-sigmoid activation functions are used for the hidden layers, and a purely linear activation function for the output layer is employed.

Each of the ANN for each of the reactive scalars in a particular temperature zone takes the species concentrations and temperature as an input, and predicts the change in the scalar normalized by the time step. It has been observed that the training provides more accurate networks with the training output being increments in the reactive scalars rather than with the final value of the scalars.[13] Figure 2 shows the off-line ANN predictions for $CH_4$ and temperature from one particular temperature regime. As can be seen, the ANN predicted values are in excellent agreement with the desired target values.

The 5-species LANN obtained here for $\phi$=1, T=300K and P=1 atm, is also used in a 2D-DNS simulation with a stationary premixed flame-turbulence interaction. Flame-turbulence studies using detailed kinetics have been reported in the past[24,25] in literature and serves as a test problem here to evaluate the LANNs. A two-dimensional domain of size $2.5 \times 2.5$ cm is resolved using a $400 \times 400$ grid points is chosen for the simulation. The simulations are performed using a finite-volume scheme that is nominally second order in both space and time. A fourth-order accurate version is also available but is not used at present since the resolution is sufficient to address the accuracy of the LANN. Characteristic inflow-outflow boundary conditions[26] are used at the inlet and outlet of the domain. Periodic boundary conditions are imposed on the other domain boundaries. An inflow velocity is prescribed equal to the laminar flame speed $S_L$. A fluctuating isotropic turbulent field with an intensity $u'$, generated based on a prescribed energy spectrum[27] also is initialized. For the conditions simulated here, $S_L = 40$ cm/s and $u' = 1.77$ m/s, and thus, $u'/S_L = 4.4$ which indicates that flame is in the flamelet regime.

Figure 3 show some instantaneous results obtained from the LANN predictions. Figure 4 shows the 1D time-averaged profiles in the middle plane from these simulations. Clearly, both direct integration (DI) and ANN predictions are in excellent agreement.

*Reduced four-step kinetics*

A reduced methane-air combustion system[17] involving 8-species ($CH_4$, $H_2$, $O_2$, $H$, $CO$, $CO_2$, $H_2O$ and $N_2$) and four steps is next considered. The mechanism is summarized in the Appendix. The methodology used earlier is followed for the development of the neural networks for this mechanism as well. Each ANN is again a three-layer Levenberg-Marquardt back-propagation network, with 20-30 neurons in the two hidden layers. Tan-sigmoid activation functions are used for the hidden layers, and a purely linear activation function for the output layer. Therefore, this LANN is quite similar to the earlier 5-species LANN, with the exception of more number of ANNs for each of the reactive scalars. This is justified, since the mechanism is more complicated and involves more number of species as an input to the ANNs.

A DNS run similar to the one for the 5-species case is performed and the results compared with DI. Figure 5 compares instantaneous $CO$ and $T$ contours in the 2D domain obtained using DI and LANN. The general shape of the wrinkled shape is nearly identical under both approaches. There are, however, some differences. This is highlighted in Figure 6 in which the time-averaged profiles for some of the scalars are shown. It is seen that although there is reasonable agreement, the flame thickness is slightly larger using LANN and as a result, the temperature is under predicted in the reaction zone. This impacts the prediction of $CO$ and other species.

Analysis suggests that the LANN output is highly sensitive for some of the radical and minor species. This is due to the presence of most of these radicals in extremely small amount and being hyper-sensitive to small changes in the local temperature. Also, the timescales of the radicals are generally much smaller than for the other species. It was determined that these discrepancies can be minimized using a simple change in the setup process. This is demonstrated below.

*Reduced five-step kinetics*

A new 9-species mechanism (see Appendix) involving $CH_4$, $H_2$, $O_2$, $OH$, $CO$, $CO_2$, $H_2O$, $NO$ and $N_2$ is investigated with the modified LANNs. We chose this mechanism instead of the earlier 8-species because it also contains $NO$ and thus, with this mechanism we can investigate the ability of LANNs to predict both $CO$ and $NO$. LANNs are built for this mechanism using the same approach as in the previous section with the exception that different transformation functions are used for different scalars. As reported above, some of the species reaction rate, which are used as an output for training, are highly sensitive to temperature changes in certain temperature regimes and insensitive in the others (see Figure 7(a)). To bring this effect into the ANN development we employ different transformations for different species, and in some cases, in different temperature range. For most of the major species, the logarithmic transformation is still employed (see Figure 7(b)) but for some of the minor species, such as $CO$ and $NO$, we employ linear transformations in some of the non-active temperature bins.

Figure 8 show the time-averaged profiles for some of the scalars as predicted using the new LANNs and compared against the DI prediction. It can be seen that the present LANN prediction is now in excellent agreement with DI results. Figure 9 show the time-averaged profiles for $CO$ and $NO$. Again, the results for this LANN are in excellent agreement with the DI results.

These results suggest that by proper mapping of the scalar-temperature space and using appropriate trans-

formations for preprocessing the network, a better ANN can be trained. These studies have demonstrated an approach that can handle both major and minor species. The computational gain using LANN is discussed later.

**Turbulent Artificial Neural Network (TANN)**

The LANN stores only the thermo-chemical composition at a point for a particular time step. Therefore, these LANNs can only be used in a DNS or in a LES where the subgrid evolution of the chemical species is closed in an exact manner.[19] For conventional LES (or for that matter, for RANS as well) obtaining the filtered reaction rate is critical for accurate predictions. However, classical models based on assumed pdfs[28] and eddy break-up[29] and eddy dissipation[30] closures have not proven very accurate in predicting pollutant emission. On the other hand, inclusion of detailed kinetics without any closure in scalar pdf methods for RANS and in subgrid linear-eddy model for LES[3] have demonstrated that improved predictions can be achieved when detailed kinetics is employed.

Application of LANNs in the subgrid LES approach[3] is currently underway to develop an efficient LES alternative for multi-component reacting flows. However, this approach is expected to be computationally expensive and therefore, will not be useful for parametric design studies using the current computer architecture. An alternate approach, denoted here as Turbulent ANN (TANN) is discussed below which attempts to develop a turbulent composition state in the combustor. In TANN, the LANN is combined with another NN for the turbulent length and velocity scales that exist locally in the combustion zone. Obviously, this NN (either independently or combined with LANN) requires the information on the turbulent fluctuations. We discuss here an approach under study.

Consider the LES-filtered species equation:

$$\frac{\partial \bar{\rho}\widetilde{Y}_m}{\partial t} + \frac{\partial}{\partial x_i}[\bar{\rho}\widetilde{Y}_m\widetilde{u}_i - \bar{\rho}\bar{D}_m\frac{\partial \widetilde{Y}_m}{\partial x_i} + \Phi^{sgs}_{i,m} + \theta^{sgs}_{i,m}] = \overline{\dot{w}}_m \quad (5)$$

The closure of the term in the right-hand-side, $\overline{\dot{w}}_m$ is very problematic. If the local joint scalar-velocity pdf, $P(Y_m, T, p, u', \Delta; x_i, t)$ can be defined, then any filtered variable can be obtained directly by integration. Here, $u'$ and $\Delta$ are respectively, the local subgrid turbulence intensity and the characteristic eddy size. We use $(u', \Delta)$ as two parameters to define the subgrid state at every LES cell. This approach is reasonable since turbulent fluctuations at a given location increase mixing due to eddies of characteristic size that ranges from the LES grid size $\overline{\Delta}$ to the smallest Kolmogorov eddy $\eta$ (thus, $\eta < \Delta < \overline{\Delta}$). Increase in mixing can increase fine-scale flame wrinkling, thereby increasing the effective burning rate.

As before, the subgrid kinetic energy is used to estimate $u'$[1] and for the subgrid Reynolds number, $Re_\Delta = u'\overline{\Delta}/\nu$ the range of eddies involved in the subgrid mixing process can be easily determined. Inertial range scaling law is employed to determine the pdf of the eddy size distribution $f(l)$. Then, given $f(l)$, $\overline{\dot{w}}_m =< \dot{w}_m >$ where $\overline{\dot{w}}_m$ is the LES filtered reaction rate (see Equation 5) and $< \dot{w}_m >$ indicates the reaction rate averaged over the local eddies. The latter term can be approximated as: $< \dot{w}_m >= \int \dot{w}_m(l) f(l) dl$, where $f(l)$ is the distribution of the length scales acting at the subgrid level. The key here is to determine $\dot{w}_m(l)$ so that effect of different eddies on the combustion process is included properly. Some recent results are discussed below.

For a 5-species global mechanism and for $\phi$=0.6, T=533K and P=5.1 atm we generate the TANN using 2D DNS simulations of the flame-turbulence interaction model described earlier. Since TANN is to be used on a coarser grid, the local combustion process in the DNS can be used to parametrize the local combustion in eddies of the smallest scales. Simulations were carried out for a range of $u'$ in a range $0 < u'/S_L < 10$ which is currently the region of interest. Note that, we are only interested in accounting for the effect of the turbulent scales that will be lost when a LES grid is used. Therefore, at this time we are considering this flame-turbulence interaction problem as a generic subgrid domain to develop the training set, and is assumed to be applicable to all fine-scale premixed flame-turbulence interactions. Thus, once the TANN is trained using this data set, then it is considered applicable in any LES configuration of interest, as long as the parameter space is similar. However, this assumption remains to be confirmed and will be the focus of future studies in this arena.

Although this approach is still under development, preliminary application of the TANN shows promise. Figure 10 shows instantaneous temperature field for the DNS (using 353x353 grid points) and the corresponding LES using TANN on a 177x177 grid resolution. As can be seen from the figures, the TANN is able to capture the overall flame-turbulence behavior. There are, however, some details that do not agree and this will be investigated further in the near future.

**Error and Efficiency Estimates**

The neural network algorithm is allowed to converge to a sufficient level of tolerance error. Mean square errors are used to define the overall network errors between the desired target value and the ANN predicted values. As has been discussed and demonstrated in the past,[18] convergence is more difficult to achieve for some of the radicals than the major species/temperature. For example, the convergence for the ANN training for a major species or temperature can be two-three times faster than that for some of the minor species training.

From an overall perspective, the ANN proves to be an excellent competitor to represent finite-rate chemistry in a turbulent flame simulation. The major advantage it has to offer is in terms of the reductions in the computational cost and memory overhead. Direct integration approaches are not always feasible, due to the enormous computational costs involved. For example, ISAT for the 9-species chemical mechanism requires around 100+ MB which has to be stored in memory to speedup access. Furthermore, as noted above, ISAT table continues to grow and therefore, memory allocation has to be dynamic and load balancing is a serious problem. On the other hand, the present ANN models (using multiple ANNs for each species and temperature) requires just around 1-2 MB of memory at most. This has significant implication for use within massively parallel systems (especially PC clusters) where the memory needs to be allocated to resolve for the flow field rather than for the chemical state.

Another issue is that ANN implementation is simple to incorporate as compared to an ISAT algorithm, involving only a few matrix multiplications and additions and floating point operations. This can significantly reduce not only the memory overheads but also the overall cost of chemical composition update. Table 1 shows the typical cost of implementing online ANN as compared to DI methods for the same (comparisons being performed on *Intel Pentium III Xeon, 500-550 MHz* machines and for a fixed number of time-steps). For the single-step mechanism the speedups are higher, since the complexity of the ANNs is increased for the multi-step mechanism. Cost reduction is expected to become more apparent for a larger chemical mechanism and when simulation is performed for multiple flow through times. This remains to be demonstrated.

## Conclusions

Artificial Neural Network has been demonstrated as a computationally economical tool for the simulation of scalar evolutions in a chemically reacting mixture. This has been shown with the aid of global single-step and reduced multi-step mechanisms. Some key issues that address the training of ANNs for major and minor species have been resolved. Application of the LANNs in DNS/LES flows show that as long as the parameter space is within the training set for the LANNs, they perform very well and at a reduced cost. From memory and storage point of view, ANN may be also a better alternative when implementing LES on massively parallel computer clusters. There are some issues still remaining to be resolved, such as, the need to generalize and/or automate the training process, the accuracy when multiple ANNs are used to cover parameter space outside the training set, etc. However, these are generalization issues and therefore, can be resolved.

Finally, as the next step for the modelling of turbulent combustion for engineering applications (i.e., to all parametric studies), the incorporation of the turbulence effects into the ANN structure have been discussed and demonstrated using TANNs. Present results obtained using TANNs are still preliminary, but they serve to validate and extend this concept. Future studies will incorporate the TANNs for the multi-step mechanism in a full-scale 3D reacting flow simulation. These results will be reported in the future.

## Acknowledgments

This work was supported in part by the Wright Patterson AFB under a subcontract from CFD Research Corporation. Computational time was provided by DOD High Performance Computing Centers at NAVO (MS), ERDC (MS) and ASC (OH).

## References

[1] Kim, W., Menon, S., and Mongia, H., "Large Eddy Simulations of a Gas Turbine Combustor Flow," *Combustion Science and Technology*, Vol. 143, 1999, pp. 25–62.

[2] Kim, W.-W. and Menon, S., "Numerical Modeling of Turbulent Premixed Flames in the Thin-Reaction-Zones Regime," *Combustion Science and Technology*, Vol. 160, 2000, pp. 119–150.

[3] Chakravarthy, V. and Menon, S., "Large-Eddy simulations of turbulent premixed flames in the flamelet regime," *Combustion Science and Technology*, Vol. 162, 1999, pp. 175–222.

[4] Stone, C. and Menon, S., "Parallel Simulations of Swirling Turbulent Flames," *Journal of Supercomputing (to appear)*, 2002.

[5] Peters, N., *Turbulent Combustion*, Cambridge Monographs on Mechanics, 2000.

[6] Maas, U. and Pope, S., "Laminar Flame Calculations using Simplified Chemical Kinetics based on Intrinsic Low-Dimensional Manifolds," *Proceedings of the Combustion Institute*, Vol. 25, 1994, pp. 1349–1356.

[7] Chen, J. Y., Kollmann, W., and Dibble, R. W., "Pdf Modeling of Turbulent Nonpremixed Methane Jet Flames," *Combustion Science and Technology*, Vol. 64, 1989, pp. 315–346.

[8] Pope, S., "Computationally Efficient Implementation of Combustion Chemistry Using *In Situ* Adaptive Tabulation," *Combustion Theory Modelling*, Vol. 1, 1997, pp. 41–63.

[9] Taing, S., Masri, A., and Pope, S., "PDF Calculations of Turbulent Nonpremixed Flames of H2/CO2 using Reduced Chemical Mechanisms," *Combustion and Flame*, Vol. 95, 1993, pp. 133–150.

[10] Christo, F., Masri, A., Nebot, E., and Pope, S., "An integrated PDF/Neural Network Approach for Simulating Turbulent Reacting Systems," *Proceedings of the Combustion Institute*, Vol. 26, 1996, pp. 43–48.

[11] Christo, F., Masri, A., and Nebot, E., "Artificial Neural Network Implementation of Chemistry with pdf Simulation of H2/CO2 Flames," *Combustion and Flame*, Vol. 106, 1996, pp. 406–427.

[12] Blasco, J., Fueyo, N., Dopazo, C., and Ballester, J., "Modelling the Temporal Evolution of a Reduced Combustion Chemical System With an Artificial Neural Network," *Combustion and Flame*, Vol. 113, 1998, pp. 38–52.

[13] Blasco, J., Fueyo, N., Larroya, J., Dopazo, C., and Chen, J., "A Single-step Time-integrator of a Methane-air Chemical System Using Artificial Neural Networks," *Computers and Chemical Engineering*, Vol. 23, 1999, pp. 1127–1133.

[14] Chen, J.-Y., Blasco, J., Fueyo, N., and Dopazo, C., "An Economical Strategy for Storage of Chemical Kinetics : Fitting In Situ Adaptive Tabulation with Artificial Neural Networks," *Proceedings of the Combustion Institute*, Vol. 28, 2000, pp. 115–121.

[15] Sankaran, V. and Menon, S., "Structure of Premixed Turbulent Flames in the Thin-Reaction-Zones Regime," *Proceedings of the Combustion Institute*, Vol. 28, 2000, pp. 203–209.

[16] Haykin, S., "Neural Networks: A Comprehensive foundation," *Neural Networks: A Comprehensive foundation*, Prentice Hall, Hamilton, Ontario, Canada, 1999, pp. 2–2.

[17] Mauss, F. and Peters, N., "Reduced Kinetic Mechanisms for Applications in Combustion Systems," *Lecture Notes in Physics 360*, edited by N. Peters and B. Rogg, Springer-Verlag, 1993, pp. 64–81.

[18] Kapoor, R., Lentati, A., and Menon, S., "Simulations of Methane-Air Flames using ISAT and ANN," *AIAA Paper No. 2001-3847*, 2001.

[19] Kapoor, R. and Menon, S., "Computational Issues for Simulating Finite-Rate Kinetics in LES," *ASME TURBO EXPO 2002 Paper No. GT-2002-30808*, 2002.

[20] Beale, M. and Demuth, H., "Neural Network Toolbox," *Neural Network Toolbox*, The Math Works, Inc., Natick, MA, 1998, p. 5.25.

[21] Moller, M., "A Scaled Conjugate Gradient Algorithm for Fast Supervised Learning," *Neural Networks*, Vol. 6, 1993, pp. 525–533.

[22] Hagan, M. and Menhaj, M., "Training Feedforward Networks with the Marquardt Algorithm," *IEEE Transactions on Neural Networks*, Vol. 5, No. 6, 1994, pp. 989–993.

[23] Westbrook, C. K. and Dryer, F. L., "Simplified Reaction Mechanisms for the Oxidation of Hydrocarbon Fuels in Flames," *Combustion Science and Technology*, Vol. 27, 1981, pp. 31–43.

[24] Baum, M., Poinsot, T. J., Haworth, D. C., and Darabiha, N., "Direct Numerical Simulation of $H_2/O_2/N_2$ Flames With Complex Chemistry in Two-Dimensional Turbulent Flows," *Journal of Fluid Mechanics*, Vol. 281, 1994, pp. 1–32.

[25] Echekki, T. and Chen, J. H., "Unsteady Strain Rate and Curvature Effects in Turbulent Premixed Methane-Air Flames," *Combustion and Flame*, Vol. 106, 1996, pp. 184–202.

[26] Poinsot, T. and Lele, S., "Boundary Conditions for Direct Simulations of Compressible Viscous Flow," *Journal of Computational Physics*, Vol. 101, 1992, pp. 104–129.

[27] Herring, J. R., Orszag, S. A., Kraichnan, R. H., and Fox, D. G., "Decay of Two-Dimensional Homogeneous Turbulence," *Journal of Fluid Mechanics*, Vol. 66, 1974, pp. 417–444.

[28] Cook, A. and Riley, J., "A Subgrid Model for Equilibrium Chemistry in Turbulent Flows," *The Physics of Fluids*, Vol. 6, No. 8, 1994, pp. 2868–2870.

[29] Fureby, C. and Löfström, C., "Large-Eddy Simulations of Bluff Body Stabilized Flames," *Proceedings of the Combustion Institute*, Vol. 25, 1994, pp. 1257–1264.

[30] Magnussen, B. F. and Hjertager, B. H., "On Mathematical Modeling of Turbulent Combustion with Special Emphasis on Soot Formation and Combustion," *Sixteenth Symposium (International) on Combustion*, 1976, pp. 719–729.

## Appendix

**8-species, 4-Step Reduced $CH_4$-air Mechanism**

$$\begin{aligned} CH_4 + 2H + H_2O &\rightleftharpoons CO + 4H_2 \\ CO + H_2O &\rightleftharpoons CO_2 + H_2 \\ 2H + M &\rightleftharpoons H_2 + M \\ O_2 + 3H_2 &\rightleftharpoons 2H + 2H_2O \end{aligned} \tag{6}$$

**Table 1 Speedups obtained using ANN [CPU time per step (sec.)]**

| | DI cost (x) | ANN cost (y) | Speedup (x/y) |
|---|---|---|---|
| 5-species, 1-step | 1.50 | 0.073 | 20 |
| 8-species, 4-step | 4.76 | 0.48 | 10 |
| 9-species, 5-step | 4.31 | 0.37 | 11 |

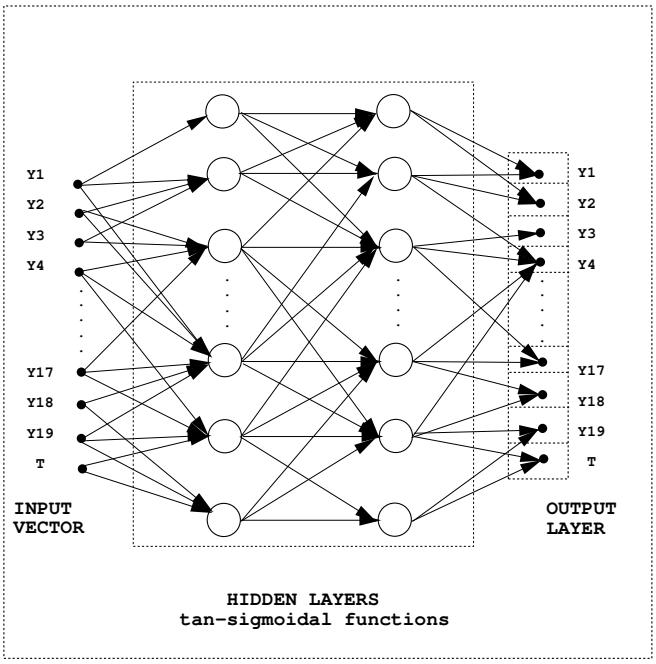


**Fig. 1 A three-layer neural network structure**

**9-species, 5-Step Reduced $CH_4$-air Mechanism**

$$
\begin{aligned}
4OH &\rightleftharpoons O_2 + 2H_2O \qquad (7)\\
2OH + 0.33CH_4 &\rightleftharpoons 1.67H_2O + 0.33CO\\
H_2 + 0.33CO &\rightleftharpoons 0.33H_2O + 0.33CH_4\\
H_2 + 4OH + 0.33CO + N_2 &\rightleftharpoons 2.33H_2O + 0.33CH_4\\
&\quad +2NO\\
2OH + CO &\rightleftharpoons H_2O + CO_2
\end{aligned}
$$

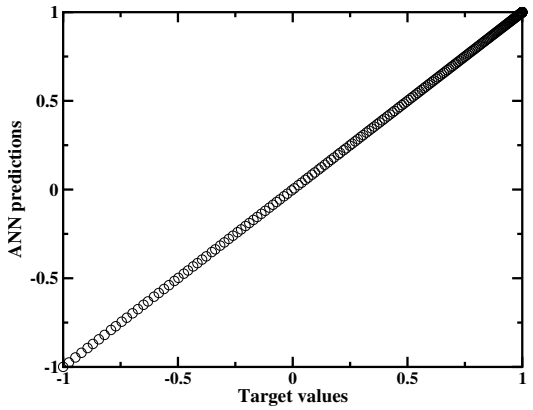


**a)** $CH_4$

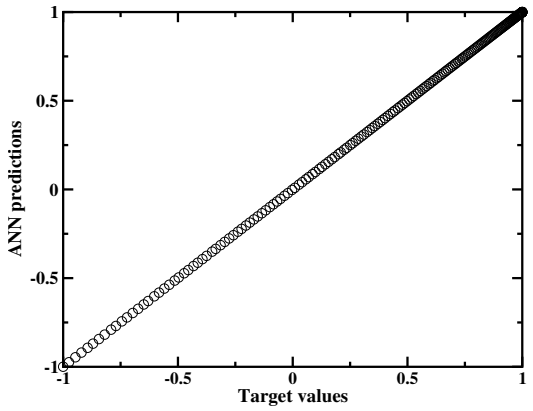


**b)** Temperature

**Fig. 2 ANN predictions for reactive scalars (5-species, single-step kinetics)**

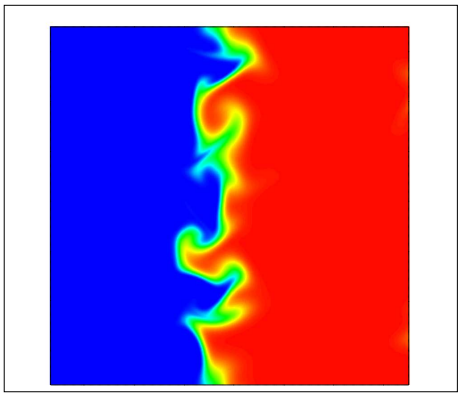

**a)** Temperature (2116K-300K)

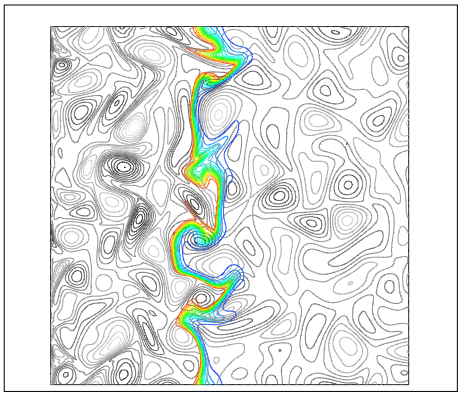

**b)** Density (colored) and vorticity

**Fig. 3 Instantaneous flame-turbulence features using LANN for single-step kinetics**

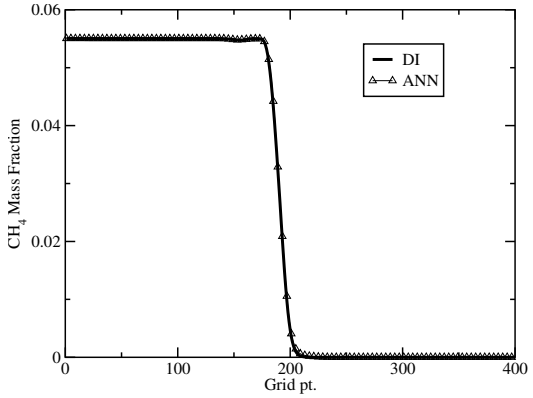


**a)** $CH_4$

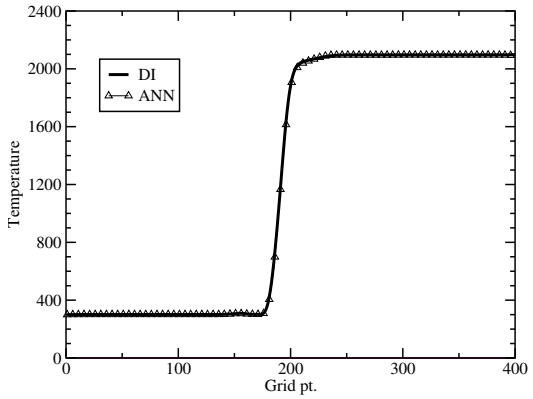


**b)** Temperature

**Fig. 4 Time averaged profiles for LANN and DI (5-species, single-step kinetics).**

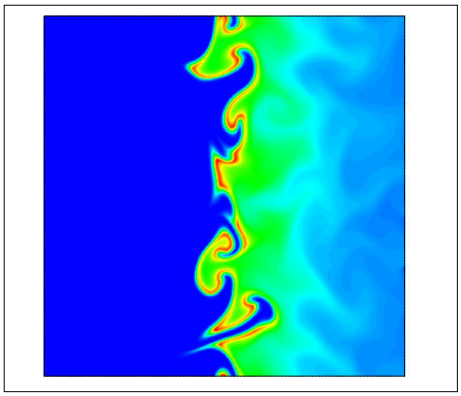

**a)** $CO$ Mass fraction (0.06-0.0), DI

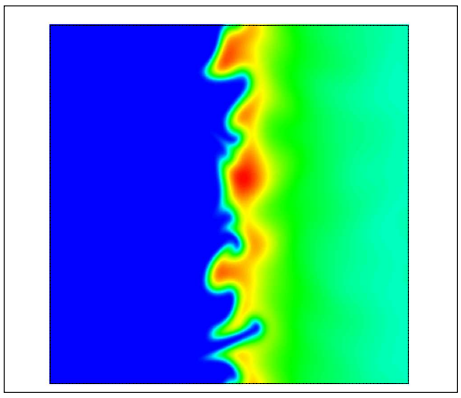

**b)** $CO$ Mass fraction (0.028-0.0), LANN

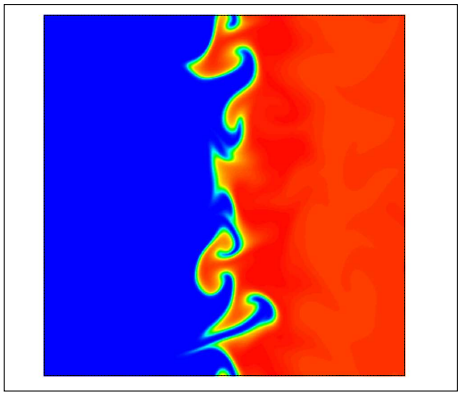

**c)** Temperature (2248K-300K), DI

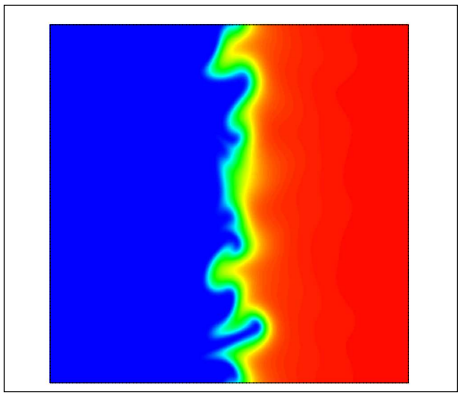

**d)** Temperature (2241K-300K), LANN

**Fig. 5 Flame turbulence interactions for DNS using 8-species, 4-step kinetics).**

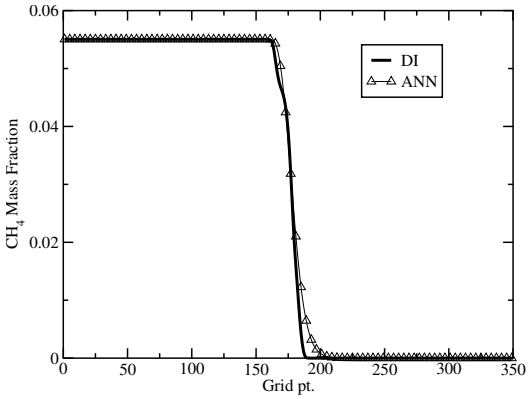


**a)** $CH_4$

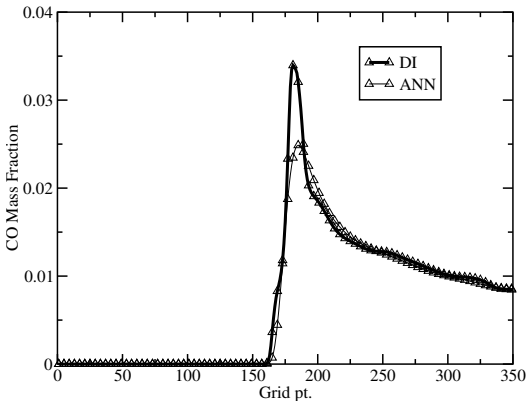


**b)** $CO$

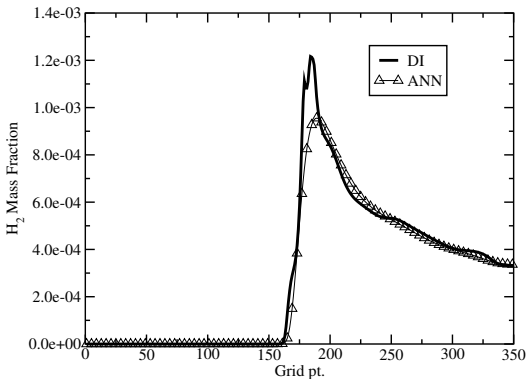


**c)** $H_2$

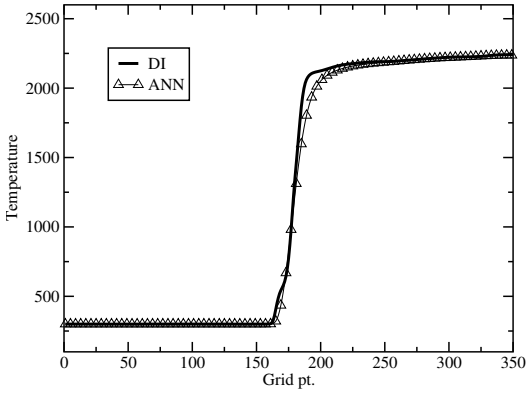


**d)** Temperature

**Fig. 6 Time averaged profile comparisons for LANN v/s DI (8-species, reduced 4-step kinetics).**

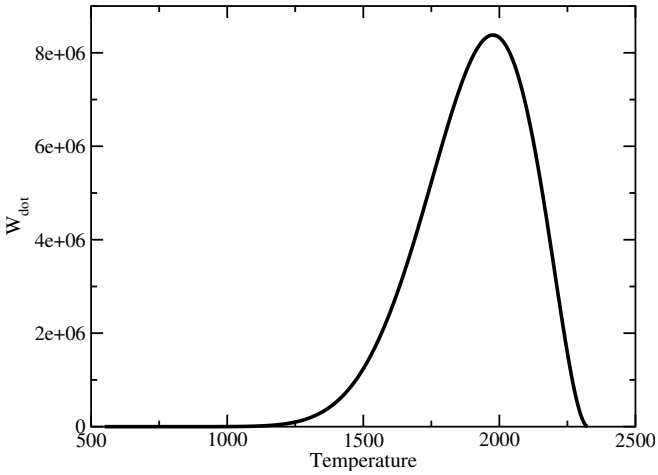


**a)** Regular

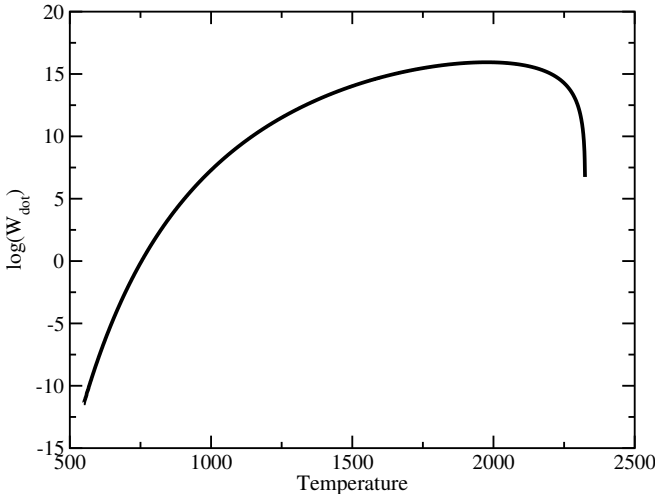


**b)** After logarithmic transformation

**Fig. 7 Effect of transformation on the production rate for a reactive scalar.**

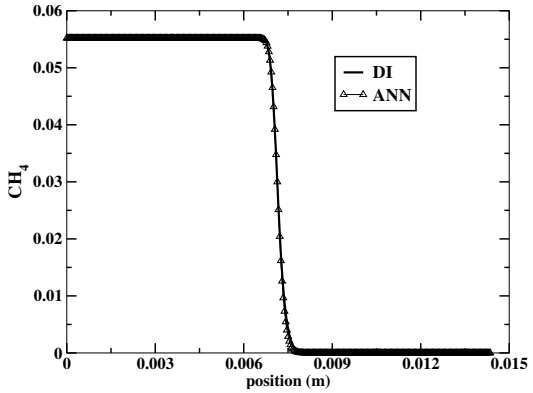


**a)** $CH_4$

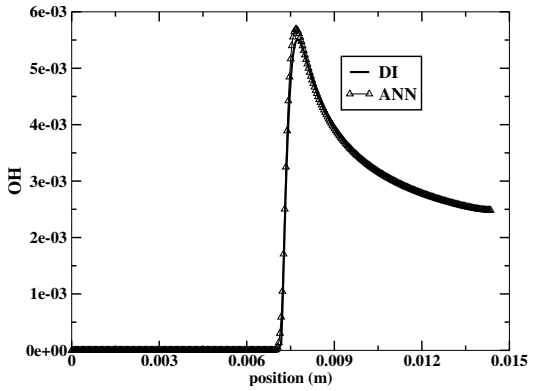


**b)** $OH$

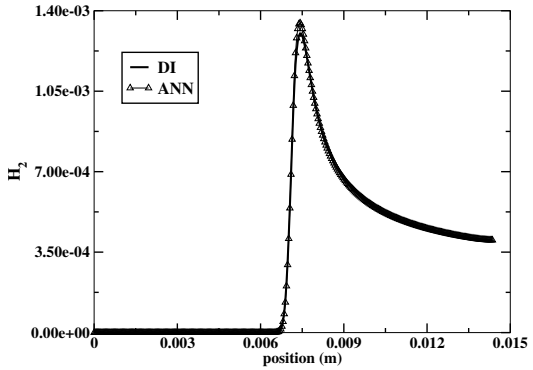


**c)** $H_2$

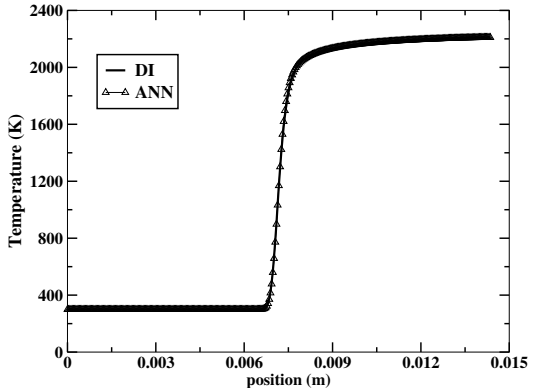


**d)** Temperature

**Fig. 8 Time averaged profile for LANN and DI (29-species, 5-step kinetics).**

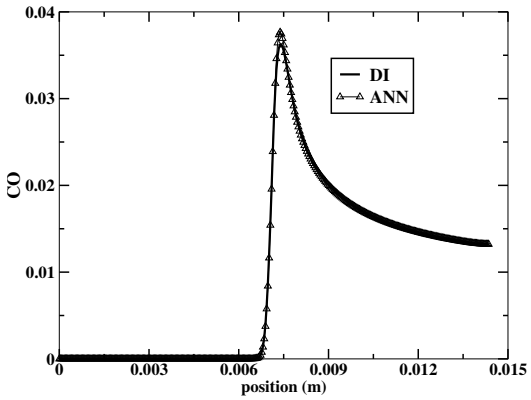


**a)** *CO*

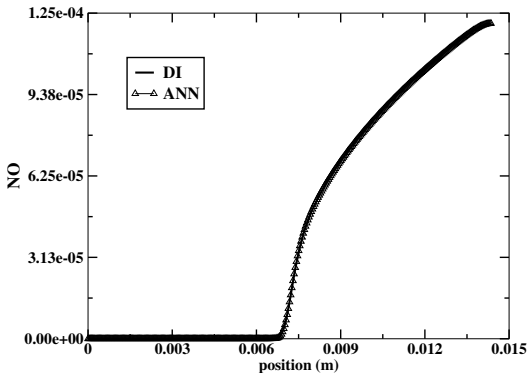


**b)** *NO*

**Fig. 9 Time averaged profiles for LANN and DI (9-species, 5-step kinetics).**

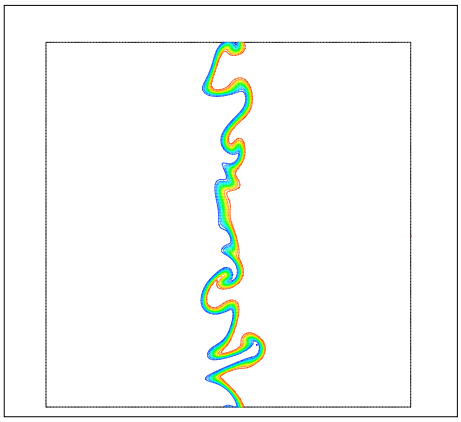

**a)** 1912K-533K, DI

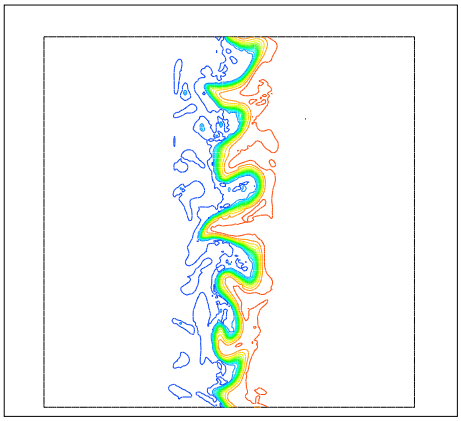

**b)** 1911K-533K, TANN

**Fig. 10 Temperature prediction using a TANN for the 5-species, single-step kinetics.**